Hindawi
International Journal of Photoenergy
Volume 2021, Article ID 8813717, 16 pages
https://doi.org/10.1155/2021/8813717

*Research Article*

# Investigation on Photovoltaic Array Modeling and the MPPT Control Method under Partial Shading Conditions

**Jianbo Bai**,[1] **Leihou Sun**,[1] **Rupendra Kumar Pachauri**,[2] **and Guangqing Wang**[1]

[1]*College of Mechanical and Electrical Engineering, Hohai University, 200# Jinling Beilu, Changzhou, 213022 Jiangsu, China*
[2]*Department of Electrical and Electronics Engineering, University of Petroleum & Energy Studies, Dehradun, India*

Correspondence should be addressed to Jianbo Bai; bai_jianbo@hotmail.com

Received 5 July 2020; Accepted 1 February 2021; Published 25 February 2021

Academic Editor: Francesco Riganti-Fulginei



On the basis of a five-parameter photovoltaic (PV) mathematical model, a multipeak output model of a PV array under partial shading conditions (PSCs) is obtained by MATLAB simulation. Simulation and experimental results demonstrate that the model can simulate the performance curves of the PV array under the PSCs. Optimized particle swarm optimization (OPSO) is used to control the multipeak output model that can quickly and accurately track the global maximum power point (GMPP) of PV modules under PSCs. Its main idea is to determine the initial position of particles and remove the acceleration factor and random number in traditional particle swarm optimization (PSO) algorithm. Additionally, according to the distance between two consecutive peak points, the maximum value of velocity is obtained. The advantages of the OPSO include the following: compared with the traditional PSO algorithm, the computing time is greatly shortened; and it is easy to achieve the MPPT with a low-cost microprocessor. In addition, a PV optimizer is designed to improve the output power of PV modules under PSCs, and simulation and experimentation have compared the output characteristics of PV modules in traditional control mode and optimized control mode under PSCs. The experimental results show that the PV optimizer improves the output power of the PV modules by 13.4% under the PSC.

## 1. Introduction

The economic requirements of PV power plants have increased with the development of science and technology. At this stage, partial shading is the main problem that reduces the economy of PV power plants as it causes a certain amount of energy loss in PV power plants [1, 2].

Partial shading may be caused by factors such as snow, tree shadows, moving clouds, and bird droppings that cover the surface of the PV module. House-integrated PV systems may have PV modules installed in different directions to fit the roof so that each panel receives a different level of irradiance, resulting in a similar effect to partial shading. Partial shading not only reduces the output power of PV modules but can also cause reversing of the polarity of solar cells and act as an external load that consumes the power generated by other solar cells, resulting in hot spots for PV cells and permanent damage to PV modules [3]. Therefore, it is necessary to avoid excessive power loss and increase the output power of PV systems by eliminating or reducing the mismatch losses caused by partial shading. The electrical energy generated by solar PV modules varies with the weather conditions. Whether a PV system operates at the maximum power point (MPP) is critical to improving its power generation efficiency. To ensure that a solar PV array works at the MPP under uniform irradiance, several MPPT methods have been implemented, such as perturb and observe (P&O) [4, 5], incremental conductance (INC) [5, 6], constant voltage (CV) [7], fractional open-circuit voltage (FOCV) [8], and fractional short-circuit current (FSCC) [9]. However, when the PV array receives nonuniform solar radiation (due to dust, surrounding buildings, clouds, trees, or utility poles), its output will have multiple local and global maxima points [10–12]. At this time, the global maximum power point (GMPP) of the PV system may be located at the first extreme point, the second extreme point, or the third extreme point so that traditional methods (such as P&O and INC) are unable to track the actual MPP under PSCs [5, 13]. In fact, under

PSCs, the power loss of a commercial PV power generation system can be as high as 70% [14]. In order to track the GMPP under PSCs, many other methods have been proposed. In two studies [15, 16], modified INC algorithms that can track the GMPP were presented, but they require a significant number of PV panels, as well as the open-circuit voltage and short-circuit current of each PV panel.

Intelligence-based MPPT algorithms were introduced, such as the particle swarm optimization (PSO) [17, 18], cuckoo search (CS) [19], firefly algorithm (FA) [20], grey wolf optimization (GWO) [21], differential evolutionary (DE) [22], genetic algorithm (GA) [23, 24], memetic reinforcement learning (MRL) [25], dynamic leader based collective intelligence (DLCI) [26], and memetic salp swarm algorithm (MSSA) [27]. The PSO has been widely used for GMPPT due to the simplicity of its mathematical structure, ease of implementation, fast computation, and strong adaptability under climatic conditions [17, 18]. An improved PSO algorithm has been developed in [17], which can find the GMPP with an accuracy of 99%. A modified particle velocity-based PSO algorithm was proposed, which solves the problems of the particle oscillation in the global best position and particle plunging into the local minima [18]. However, these PSO algorithms do not include the initial position of the particles and the random numbers, which are critical to the number of iterations the PSO algorithm uses to track the GMPP and help it avoid falling into the local minima. These PSO algorithms define the initial position of the particles by random numbers, which reflects the randomness of the PSO, but this randomness has certain problems. When the initial position of the particle is far away from the GMPP, this will increase the number of iterations. When the initial position of the particle is distributed near a local peak, the MPP of the MPPT will fall into the local part, which will cause a waste of PV modules' output power. In addition, the search efficiency of these PSO algorithms will be significantly reduced due to the random number. In the process of searching the GMPP, only a small change in the velocity of the PSO equation can be acquired when a low-value random number is multiplied with the duty cycle. Therefore, more iterations are needed. If the value of random number is too large, it may cause the MPPT to escape from the GMPP and fall into a local peak.

Furthermore, hybrid MPPT methods have been developed to improve the performance of the above methods, such as the modified P&O with an artificial neural network (MP&O-ANN) [28], overall distribution with PSO (OD-PSO) [29], differential evolutionary with PSO (DE-PSO) [30], P&O with PSO (P&O-PSO) [31], grey wolf optimization with P&O (GWO-P&O) [32], incremental conductance with firefly algorithm (INC-FA) [33], and cuckoo search with golden section search (CS-GSS) [34]. These methods can find the GMPP, but they are algorithmically complex and have a long computing time.

Motivated by the imperfection of these existing MPPT methods, an optimized particle swarm optimization (OPSO) is proposed in this study to track the GMPP for a PV system under PSCs. The novelty of this study is as follows:

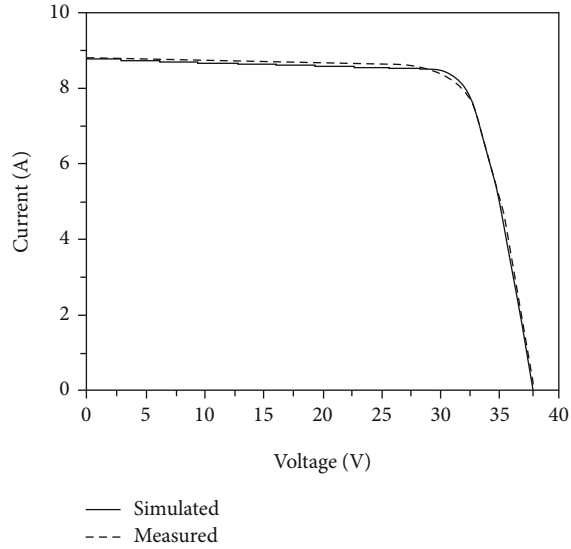


Figure 1: TSM-240PC05 $I - V$ curves under STCs.

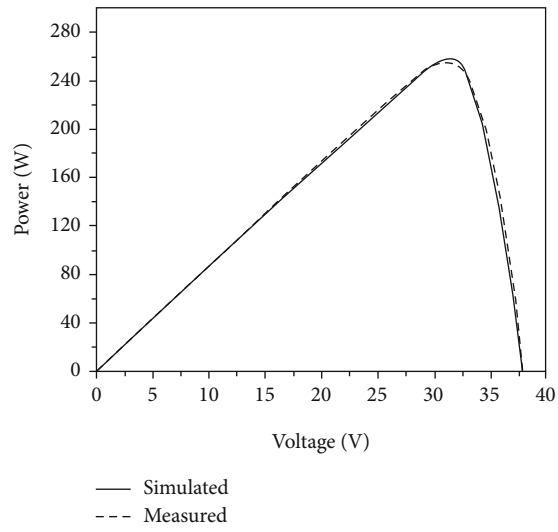


Figure 2: TSM-240PC05 $P - V$ curves under STCs.

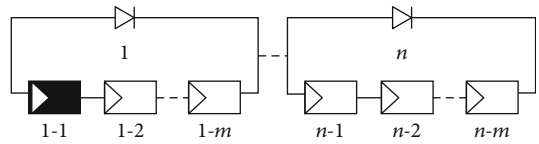


Figure 3: Schematic diagram of a shaded cell in a PV module [36].

(i) On the basis of a five-parameter PV mathematical model, a multipeak output of a PV array under PSCs is obtained by MATLAB simulation

(ii) An OPSO algorithm is proposed to realize the control of the GMPP under multipeak conditions by optimizing the initial position and inertia of the particle, which can reduce the number of iterations the traditional PSO algorithm uses to

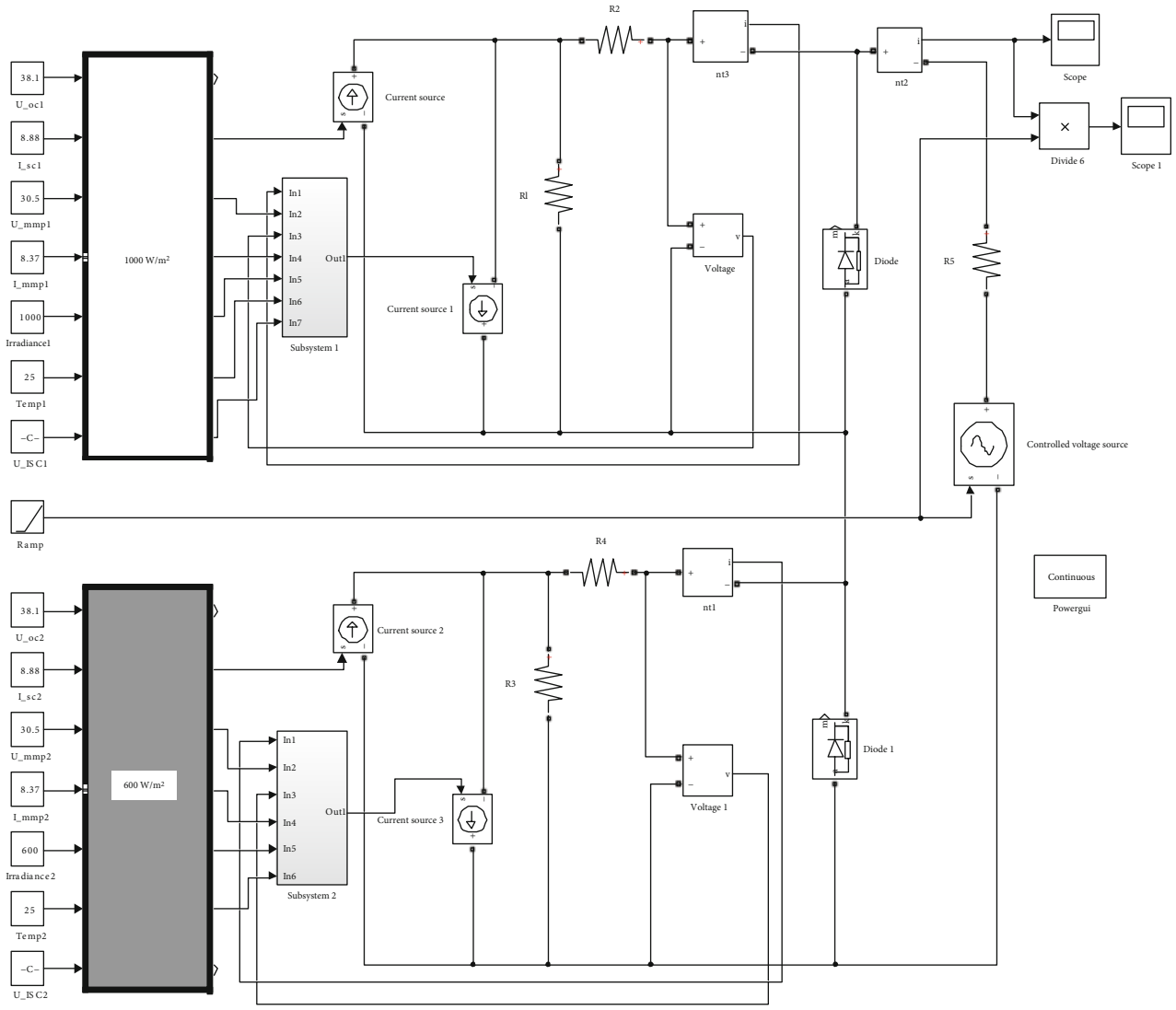


Figure 4: PV array simulation model under PSCs.

track the GMPP and help it avoid falling into the local peak

(iii) The maximum value of velocity is determined, which is very useful for MPPT with the PSO algorithm. For example, weather changes cause frequent alterations in the $P-V$ curve. By controlling the maximum value of velocity, the duty cycle can be changed smoothly to realize the real-time tracking

(iv) The convergence speed of the OPSO algorithm is more than twice as fast as that of the traditional PSO algorithm when the output power of PV modules reached convergence; and it is easy to achieve the MPPT with a low-cost microprocessor

(v) A PV optimizer is designed that protects against shadow occlusion, including the hardware design and software programming. The performance of the PV optimizer was verified by simulations and experiments

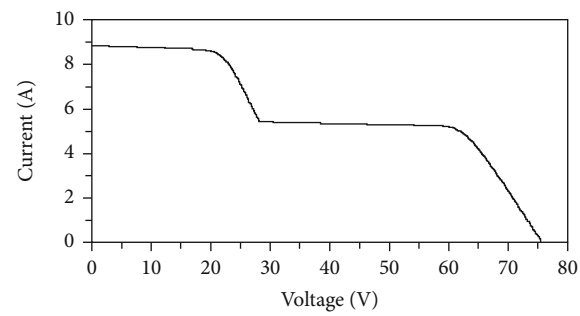


Figure 5: $I-V$ curve under the PSC.

This paper is organized as follows. Section 2 discusses the test of the five-parameter simulation model. Section 3 presents the output characteristics of the five-parameter PV array model under PSCs, and an OPSO algorithm is proposed in Section 4. Section 5 describes the PV optimizer

and optimized control method, and the control effect of the PV optimizer is verified by experiments in Section 6. Section 7 summarizes the whole paper.

## 2. Five-Parameter Simulation Model

In this study, the five-parameter model [35], which is the existing model in the authors' laboratory, is verified by simulation and experiment. Figures 1 and 2, respectively, show the $I-V$ and $P-V$ curves of the TSM-240PC05 PV module under standard conditions (STCs). After calculation, the fitting degree between the simulated data and the measured data is 99% under STCs (1000 W/m$^2$), which demonstrates that the five-parameter model has a high accuracy.

## 3. PV Module Output Characteristics under PSCs

Research on the output characteristics of PV arrays under PSCs is mainly divided into the series circuit performance study of nonbypass diode PV modules and the electrical performance of series circuits with bypass diode PV modules. Since the currently used PV modules have a bypass diode with a protection function, the electrical performance of the bypass diode series circuit is studied here. The simulation model of the PV array under the PSC is built here on the basis of the five-parameter model introduced in Section 2.

As presented in Figure 3, when the No. 1–1 cell is blocked, the $I-V$ equation of the PV array is shown in [36]

$$V = V_1 + \sum_{i=2}^{n} V_i = V_1 + (n-1) * \left(a_{cs} \ln\left(\frac{I_{ph,cs} - I}{I_{o,cs}} + 1\right) - IR_{s,cs}\right), \quad (1)$$

where $V$ is the voltage of the PV array, $V_1$ is the voltage of the No. 1 cell string, $I$ is the current of the PV array, $n$ is the number of bypass diodes, and $a_{cs}$, $I_{ph,s}$, $I_{o,cs}$, and $R_{s,cs}$ are the parameters of PV strings.

In the PV array simulation model of Figure 4, two PV panels are connected in series. During the simulation, the illumination intensity of the first PV panel is 1000 W/m$^2$, and the illumination intensity of the second PV panel is 600 W/m$^2$. In this case, the second panel is the shaded panel in the PV array. Connecting two different irradiance panels in series and bypassing parallel diodes is equivalent to the case where some cells are blocked in the same series of PV panels. The corresponding simulation results are shown in Figures 5 and 6.

Based on theoretical model analysis and model simulation, this model has been experimentally verified. The parameters of the two PV modules (TSM-240PC05) used in the experiment are shown in Table 1. One of the PV modules was shaded during the experiment. The irradiance of the first PV module was 550 W/m$^2$, and the irradiance of the second shaded PV module was 56 W/m$^2$. The ambient temperature was 25°C. Experimental data was collected on a 6952A portable solar cell tester. The experimental process picture is shown in Figure 7. The comparison of the simulated and measured data is shown in Figures 8 and 9.

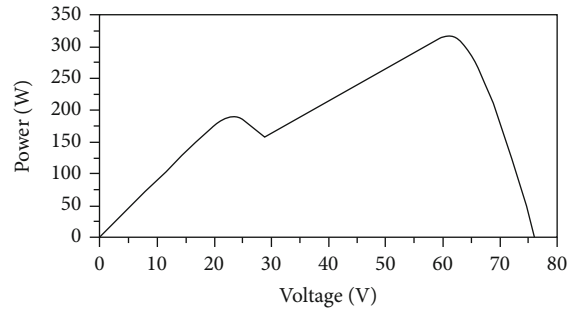


Figure 6: $P-V$ curve under the PSC.

Table 1: Data sheet of PV module (model: TSM-240PC05).

| Parameters | Data |
|---|---|
| $P_m$ (W) | 265 |
| $V_m$ (V) | 31.5 |
| $I_m$ (A) | 8.37 |
| $V_{oc}$ (V) | 38.1 |
| $I_{sc}$ (A) | 8.88 |
| $\eta_m$ (%) | 15.6 |
| Number of cells | 60 pcs |
| $u_{I,sc}$ (%/°C) | 0.05% |
| $u_{V,oc}$ (%/°C) | −0.32% |
| $T_{NOCT}$ (°C) | 44 ± 2 |

Figure 7: Experimental process picture.

Through Figures 8 and 9, it can be concluded that the experimental data and the simulation data have a very high degree of fit. The performance curves of the experimental data have a few twists and turns due to the ageing and mismatch of the PV strings. It is verified that the model can simulate the output characteristics of the PV array when one of the PV modules is completely shaded.

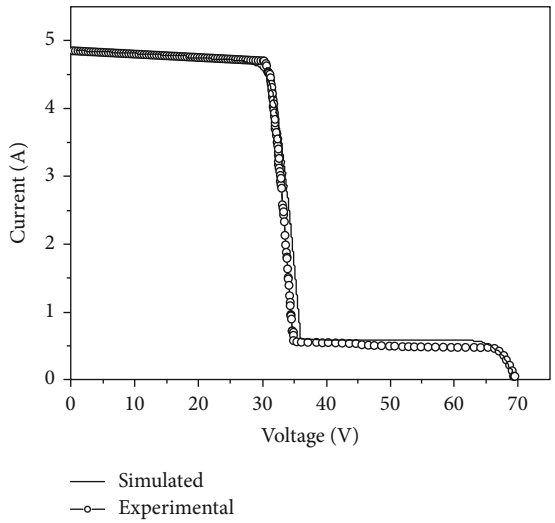


Figure 8: $I - V$ data when one of the PV modules is completely shaded.

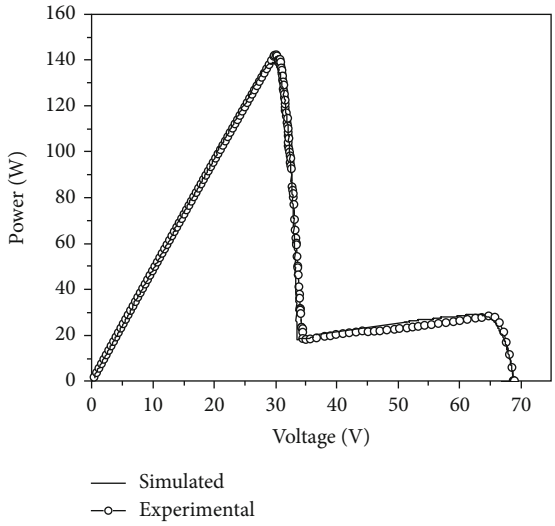


Figure 9: $P - V$ data when one of the PV modules is completely shaded.

Figure 10: Partial shading experiment.

In addition, the simulation and experiment were carried out for the case where parts of the PV panel were shaded. The experimental process was still connected in series by two PV modules (TSM-240PC05) components, and a small piece of the PV panel was blocked. This experiment mainly proves that the multipeak output model can simulate the output characteristics of the PV module when it is partially shaded. The irradiance of the PV modules was 910 W/m$^2$. The ambient temperature was 25°C. The experimental diagram is shown in Figure 10.

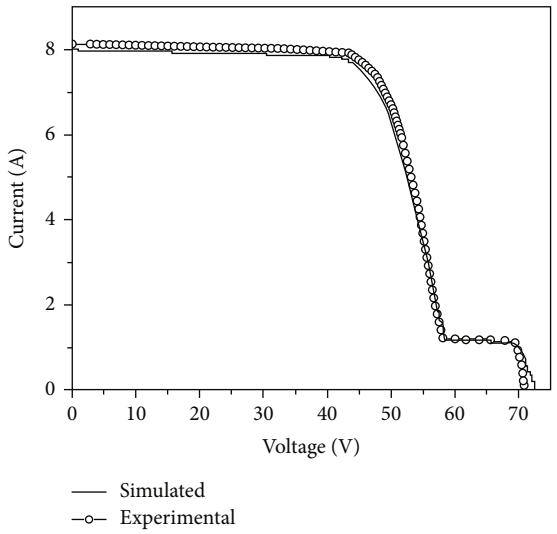


Figure 11: $I - V$ data when the PV module is partially shaded.

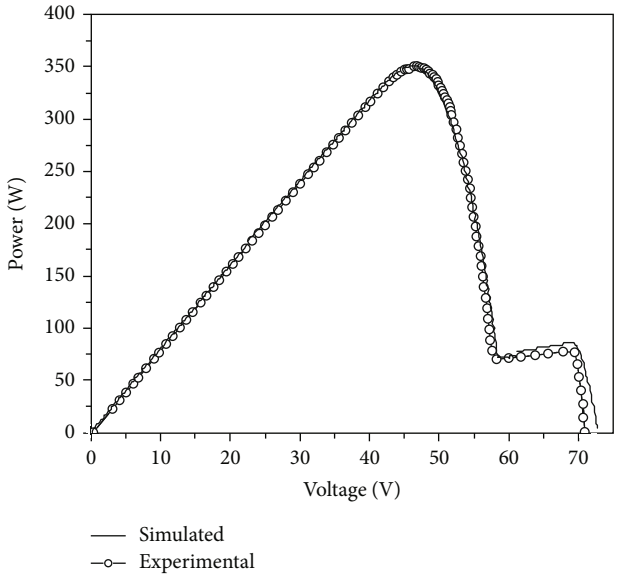


Figure 12: $P - V$ data when the PV module is partially shaded.

The analysis and sorting of the experimental data yielded the comparison between the experimental curves and the simulated curves, shown in Figures 11 and 12.

Figures 11 and 12 show that the experimental curves have a very high degree of coincidence with the simulation curves, and it is verified that the multipeak output model can

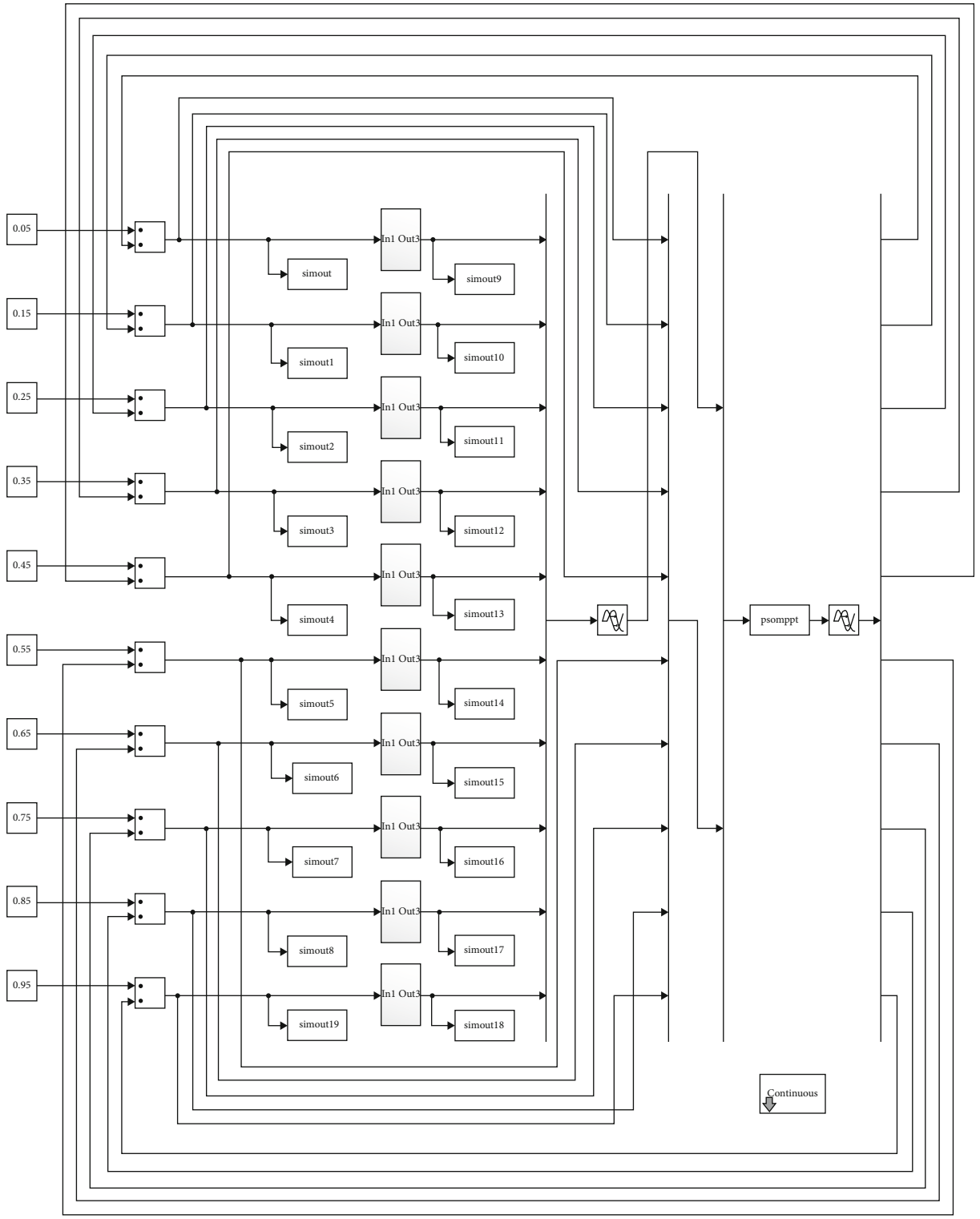


Figure 13: OPSO algorithm model for MPPT.

simulate the output characteristics of the partially blocked PV modules.

Through the verification of the above two experiments, it is found that the multipeak output model can simulate the $I - V$ and $P - V$ characteristics of PV modules under PSCs. After further calculation, the relative errors of the output power in these simulated and experimental $I - V$ and $P - V$ curves are all within 2.1%. In addition, the model does not require the solutions of nonlinear equations and the cumbersome segmentation function.

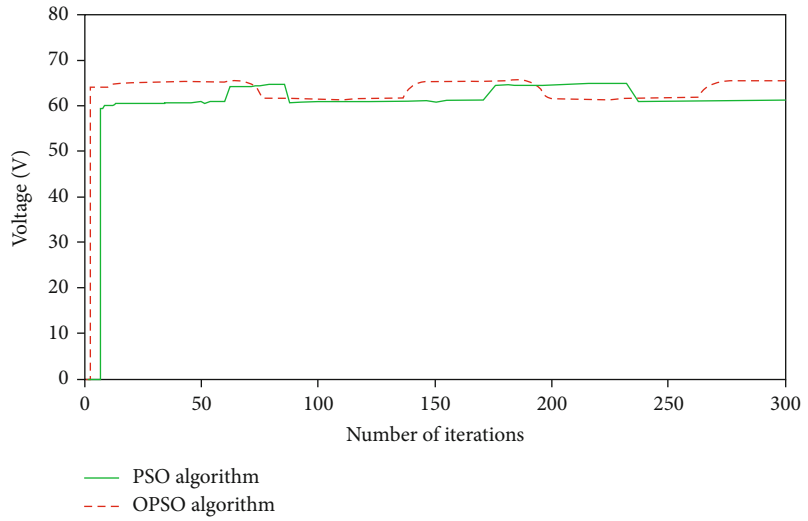


Figure 14: Comparison of the voltage convergence at the MPP between the traditional PSO algorithm and the OPSO algorithm.

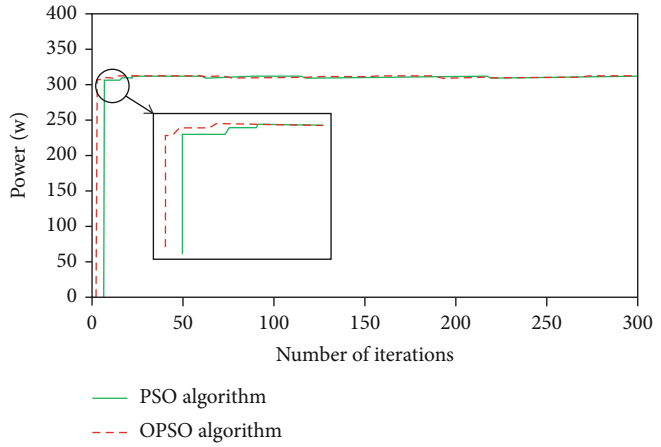


Figure 15: Comparison of the MPP convergence between the traditional PSO algorithm and the OPSO algorithm.

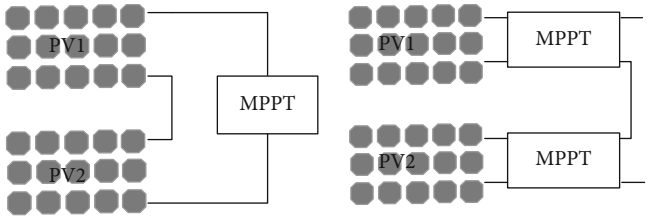


(a) Traditional MPPT control mode (b) Optimized MPPT control mode

Figure 16: Comparison of the PV array MPPT control modes.

## 4. MPPT Model of the OPSO Algorithm

The PSO algorithm is suitable for continuous function extremum problems and has a strong global search ability for nonlinear and multipeak problems. It does not need to encode and directly uses the position of the particle to represent the independent variable [37]. Speed and position updates are the core of the PSO. The principle expression and update method are as follows [38]:

$$v_{iN} = w * v_{iN} + c_1 * r_1 (P_{iN} - x_{iN}) + c_2 * r_2 (P_{gN} - x_{iN}), \quad (2)$$

$$x_{iN} = x_{iN} + v_{iN}, \quad (3)$$

where $v_{iN}$ is the particle velocity, $x_{iN}$ is the particle position, $P_{iN}$ is the best position of the individual particle, $P_{gN}$ is the best global position of the particle swarm, $w$ is an inertia weight that influences the particle velocity, and $c_1$ and $c_2$, the cognitive and social parameter, respectively, are collectively known as the acceleration coefficients. $r_1$ and $r_2$ are vectors containing random numbers generated at every iteration ($0 \le r_1, r_2 \le 1$), $i$ is the individual particle, and $N$ represents the spatial dimension (the number of independent variables).

The $P - V$ curve will have multiple peak points while the PV array is shaded. Only the peak point with the highest power among all the peak points is the MPP, and the MPPT is to find that one. When the OPSO algorithm is applied to the MPPT process, the target function is the output power $P$ of the PV array, and the position is the output voltage $V$ of the PV array, and the maximum power $P_{mp}$ is sought by continuously updating the voltage $V$.

In the process of implementing the MPPT control using the traditional PSO algorithm, the initial position of the particle needs to be defined in the first iteration (the initial value of the duty cycle needs to be defined in the control algorithm). The traditional PSO algorithm defines the initial position of the particle by a random number, which reflects the randomness of the PSO, but this randomness has certain problems. When the initial position of the particle is far away from the GMPP, this will increase the number of iterations. When the initial position of the particle is distributed near a local peak, the MPP of the MPPT will fall into the local part, which will cause a waste of PV modules' output power. Therefore, based on the optimization of the velocity factor structure, the initial position of the particle is optimized. The initial position of the particle is changed from the original random number to a fixed value. When the PSO algorithm is applied to the MPPT, the initial position of the particle is the actual duty cycle of the BOOST circuit. According to Arora [39], the duty cycle is divided into 10 equal parts; the maximum value of the duty ratio is 1, and the minimum value is 0, so the initial position of the particle is a certain value, which, in turn, reduces the randomness of the particle position of the PSO algorithm. This helps to avoid particles falling into local extremes.

Patel and Agarwal found that the distance between two consecutive peak points is about 80% of the open-circuit voltage of a PV module [40]. Therefore, by removing the random factor and the acceleration coefficient of Equation (2) and limiting the maximum value $v_{max}$ of the velocity according to the distance between the two extreme points, the velocity $v_{iN}$ is optimized. Structurally, this optimization process can delete the random number and acceleration coefficient in Equation (2). Then, the modified velocity equation of the PSO algorithm can be written as

$$v_{iN} = w * v_{iN} + (P_{iN} - x_{iN}) + (P_{gN} - x_{iN}),$$
$$|v_{iN}| \le v_{max} = 0.8 V_{oc\_module}, \tag{4}$$

where $v_{max}$ is the maximum value of velocity and $V_{oc\_module}$ is the open-circuit voltage of a single PV module.

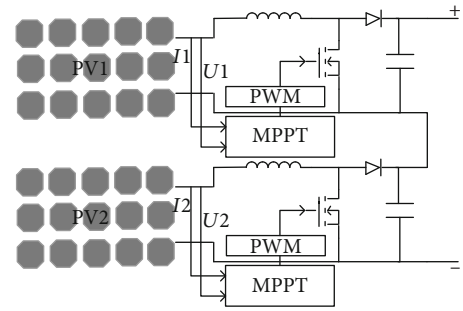


Figure 17: Optimized MPPT control mode.

According to the distance between two consecutive extreme points under PSCs, the random inertia weight (PSO-RIW) [41] is selected to update the inertia weight as follows:

$$w = 0.5 + \frac{r_m}{2}, \tag{5}$$

where $r_m$ is a random number ($0 \le r_m \le 1$). The random inertia weight strategy not only has the opportunity to get a smaller inertia weight value in the initial stage of particle operation, which is conducive to the local search, but also has the opportunity to get a larger inertia weight value in the later stage, which is conducive to increase the search intensity.

In this study, the OPSO algorithm was written in the S function, and the MPPT control model under the mismatch condition was built by SIMULINK module. The simulation model is shown in Figure 13.

In this paper, the traditional PSO algorithm and the OPSO algorithm are compared to control the MPPT. During the simulation, the multipeak output model does not change, and the initial duty cycle of the traditional PSO algorithm and the OPSO algorithm remains unchanged; only its control algorithm is changed.

The comparison of the GMPP convergence between the traditional PSO algorithm and the OPSO algorithm in the MPPT process is shown in Figure 14.

Figure 15 shows that when the output power of PV modules reached convergence, the number of iterations of the OPSO algorithm is 3 and that of the traditional PSO algorithm is 8. The convergence speed of the OPSO algorithm is more than twice as fast as that of the traditional PSO algorithm, and they have the same MPPT control accuracy. This greatly improves the real-time performance of MPPT under PSCs.

## 5. PV Optimizer Design

In the current stage of PV power plant construction, most of the PV power plants still adopt the traditional MPPT control mode, and a group of PV components shares an inverter with the MPPT function. This way, the efficiency of PV modules can be improved. However, the improved output power in this method is limited and the stability of the MPPT is low. In order to improve the output power of PV array, an

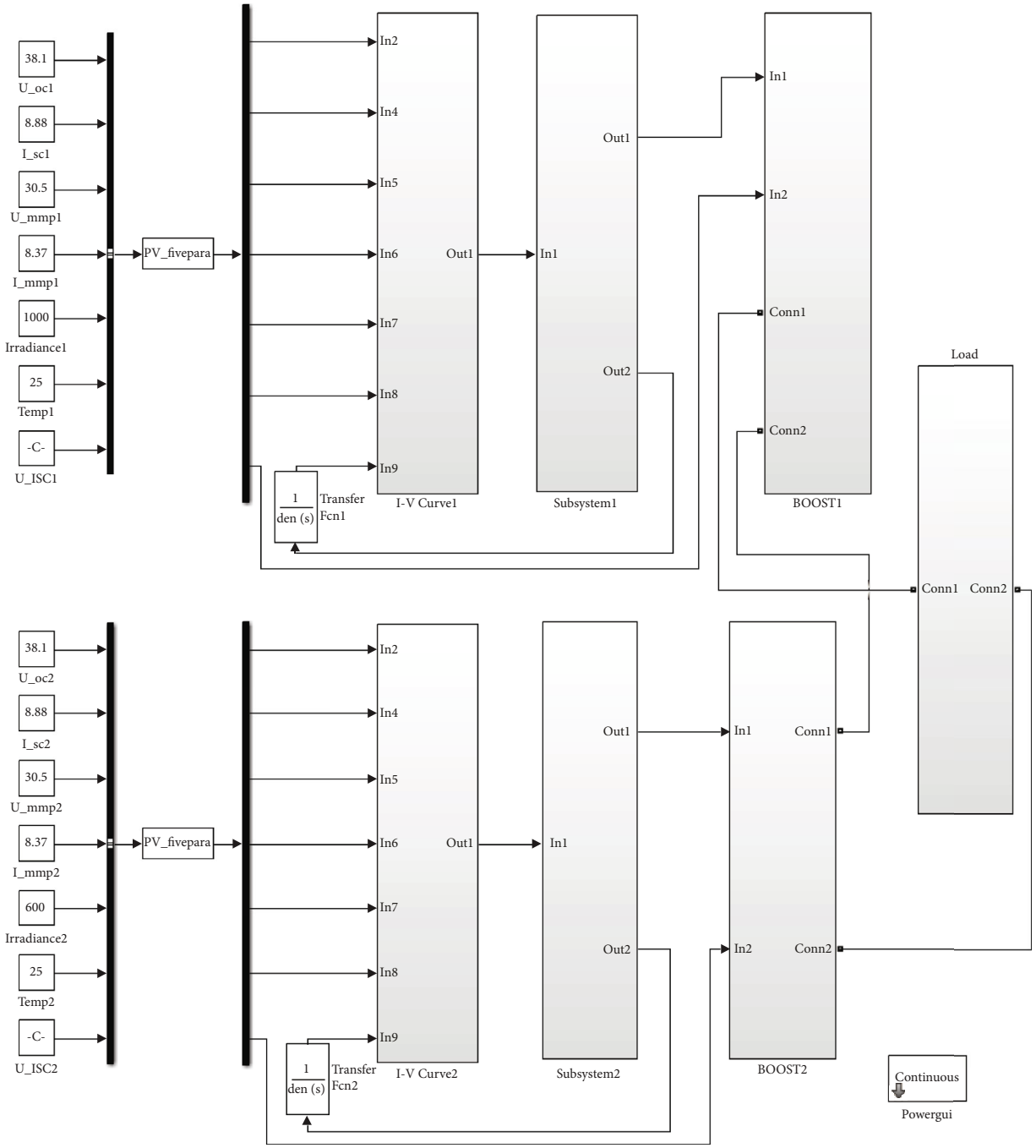


Figure 18: Simulation model of the PV optimizer.

optimized MPPT control mode using OPSO algorithm is adopted. A comparison diagram of the traditional MPPT control mode and the optimized MPPT control mode is shown in Figure 16.

In Figure 16(a), the traditional MPPT control mode is oriented to a series of PV modules in series and parallel. This MPPT control mode can achieve the MPPT of a PV array in general environments, but not when there is a complex shadow occlusion. In Figure 16(b), each PV module is connected to a PV optimizer with an MPPT controller. This MPPT control method eliminates the energy loss caused by uneven illumination and component mismatch. The optimized MPPT control mode is shown in Figure 17.

In the control schematic of Figure 17, there are two PV modules on the left and two DC-DC converters on the right. The MOSFET in the DC-DC converter is turned on/off by the PWM wave control. The duty cycle of the PWM wave is determined by the MPPT control algorithm. After the controller collects the current and voltage signals of the PV module, the duty cycle of the PWM is output through an algorithm, and then, the MPPT of the monolithic PV module is realized by the DC-DC converter.

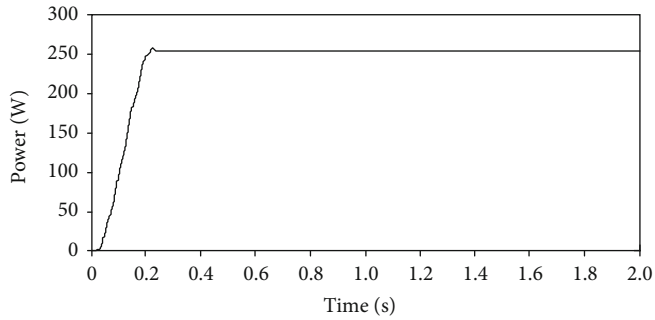


Figure 19: Output power of the PV module with an irradiance of 1000 W/m$^2$.

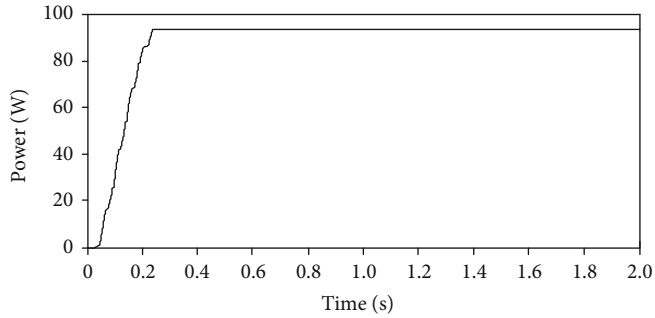


Figure 20: Output power of the PV module with an irradiance of 600 W/m$^2$.

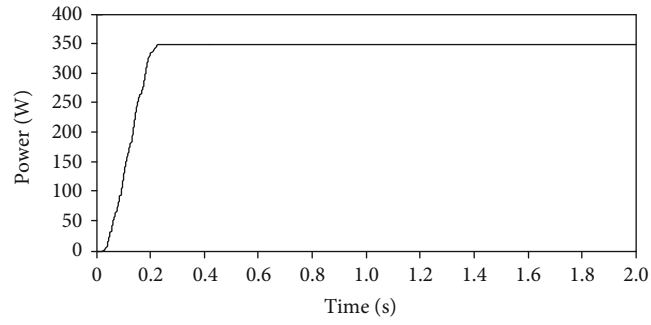


Figure 21: Output power of the two PV modules in the optimized MPPT control mode.

The PV optimizer has the effect of increasing the output power of the PV module under PSCs. The simulation model of the PV optimizer (see Figure 18) was built using MATLAB software. In this work, the two PV modules are TSM-240PC05, with irradiance of 1000 W/m$^2$ and 600 W/m$^2$, respectively. The simulation results are shown in Figures 19–21.

Figure 21 shows that in the optimized MPPT control mode, the output power of the two photovoltaic modules is 348 W, while in the traditional MPPT control mode, the output power of the two photovoltaic modules is 311 W (see Figure 6). The results show that the optimized MPPT control mode can improve the efficiency of the two PV modules by 13.4% compared with the traditional MPPT control mode.

## 6. PV Optimizer Experiment Verification

In order to verify the optimized MPPT control mode and control effect of the PV optimizer using OPSO algorithm, we build a PV optimizer system, which was mainly composed of the PV components, BOOST circuit, sampling circuit, drive circuit, and control module. In the experiment, the first part verified the efficiency of the BOOST circuit by controlling the output duty of the module, and the second part verified the improvement effect of the PV optimizer on the output power of the PV module under the shadow blocking condition. This experiment verified the performance of the PV optimizer in real time.

In this experiment, the power module was mainly used as the input, and the initial input voltage of the power module was 5.25 V. The power module was connected to the BOOST circuit and the controller output PWM signal with duty cycles of 0.3, 0.5, and 0.7 that were used to test the performance of the BOOST circuit. The physical map of the BOOST circuit is shown in Figure 22. The experimental results of the input voltage, duty cycle, and output voltage of the BOOST circuit are shown in Figure 23.

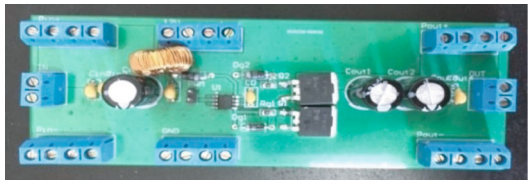

Figure 22: BOOST circuit.

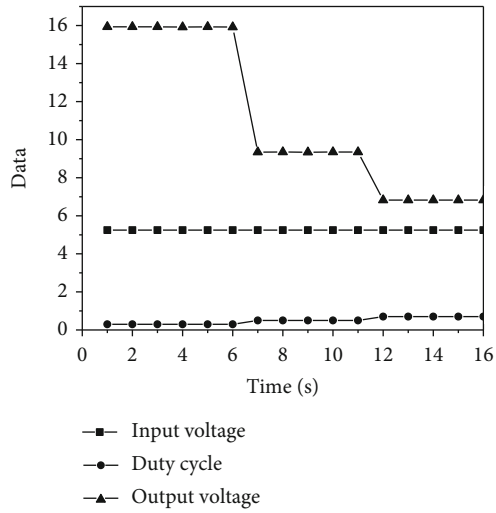


Figure 23: Relationship of input voltage, duty cycle, and output voltage.

According to the experimental results, when the input voltage is 5.25 V and the duty ratios are 0.3, 0.5, and 0.7, the output voltages of the BOOST circuit are 15.93 V, 9.3 V, and 6.827 V, respectively. The efficiency of this BOOST circuit is approximately 90%.

The experiment was conducted to verify the effect of the PV optimizer on the output power of the PV module under the shadow blocking condition. Two PV modules were used in the experiment, each of which was connected with a BOOST circuit in series. The sampling circuit fed back the collected voltage value and current value to the control system and realized the maximum output power of a single PV module through the control algorithm, improving the output power of the two PV modules. The experimental system diagram is shown in Figure 24.

The PV modules in this experiment were small size power capacity, and the solar simulator was used to provide irradiance. The data sheet of the two PV modules is shown in Table 2.

The solar simulator was a TRM-PD artificial solar simulator produced by Jinzhou Sunshine Meteorology. The solar simulator is mainly composed of three parts: a xenon tube, a control cabinet, and a lifting bracket. The spectrum of the xenon lamp is excellent, similar to the spectrum of sunlight, and it has a small volume and high luminous efficiency.

Two sets of shadow occlusion experiments were performed using the above system. Experiment 1 mainly verified the accuracy of the PV optimizer tracking the MPP in the

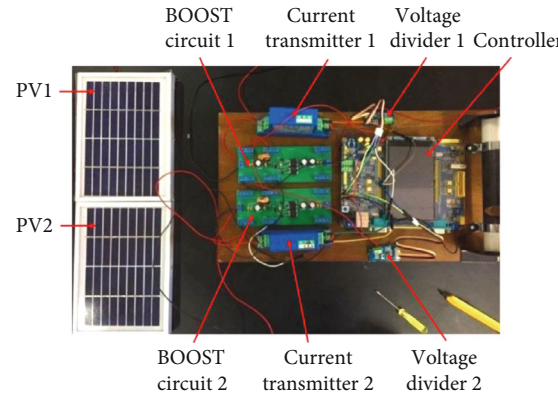


Figure 24: Experimental system.

Table 2: Data sheet of PV module.

| Parameters | Data |
|---|---|
| $P_{max}$ (W) | 2 |
| $V_{max}$ (V) | 9 |
| $I_{max}$ (A) | 0.222 |
| $V_{oc}$ (V) | 10.2 |
| $I_{sc}$ (A) | 0.233 |
| Size (mm) | 180 ∗ 130 ∗ 17 |
| Test conditions | 1000 W/m$^2$, AM 1.5, 25°C |

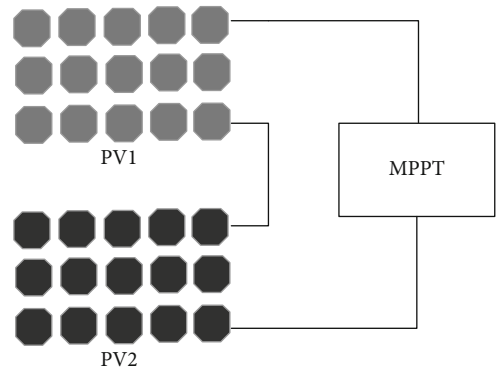


Figure 25: Shadow occlusion of the PV modules in the traditional MPPT control mode.

environment where the area of a single PV panel was blocked. Experiment 2 was a comparison of the output power between the traditional MPPT control mode and the optimized MPPT control mode.

In Experiment 1, two PV modules in series shared one BOOST circuit. The shadow blocking condition of the two PV modules and the MPPT control mode is shown in Figure 25. During the experiment, the irradiance of PV module 1 was 770 W/m$^2$, and the irradiance of PV module 2 was 475 W/m$^2$, that is, PV module 2 with a 475 W/m$^2$ irradiance was affected by shadow occlusion. The $I - V$ curve and the $P - V$ curve of the two PV modules under the PSC are plotted in Figures 26 and 27, respectively.

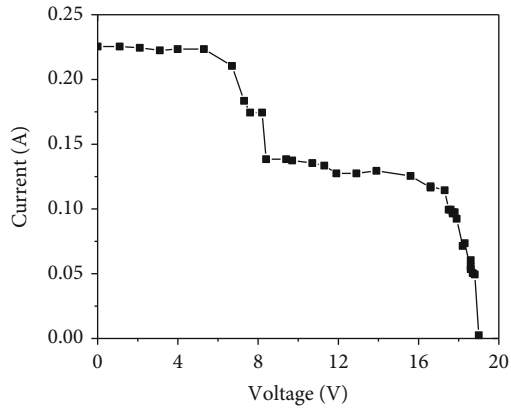


Figure 26: $I - V$ performance curve of the PV modules in the traditional MPPT control mode.

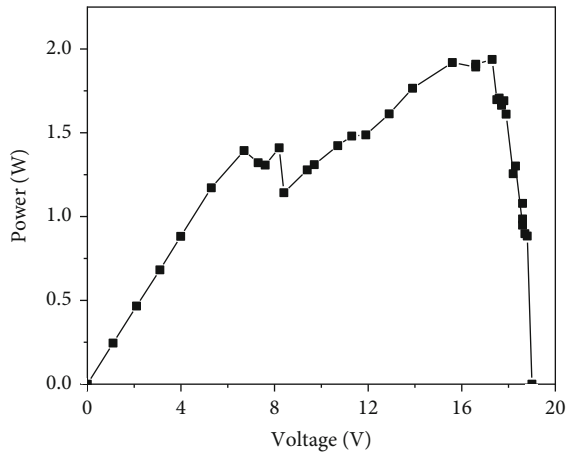


Figure 27: $P - V$ performance curve of the PV modules in the traditional MPPT control mode.

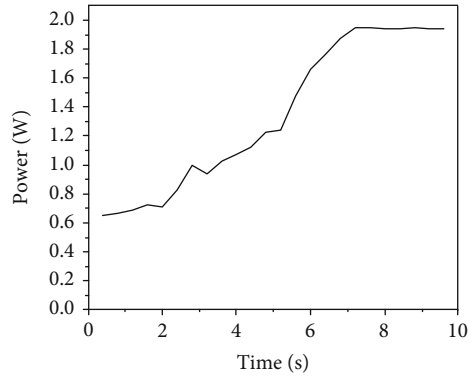


Figure 28: MPPT by the PV optimizer in the traditional MPPT control mode.

The tests have shown that the PV optimizer can efficiently monitor the MPP when the area of a single PV module is shaded. In Figure 27, the highest point power is 1.94 W, which is the maximum power of the PV module. In

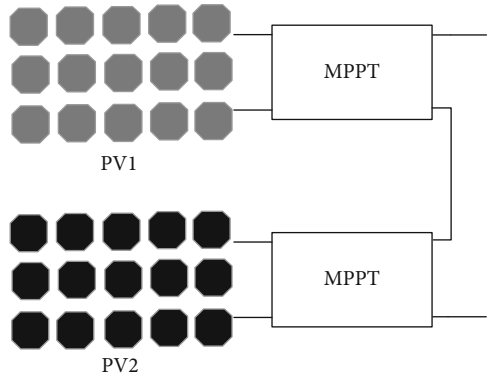


Figure 29: Shadow blocking of the PV modules in the optimized MPPT control mode.

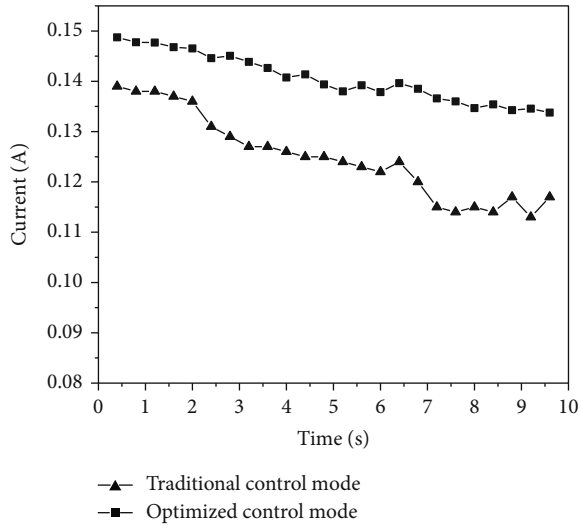


Figure 30: Current comparison during MPPT.

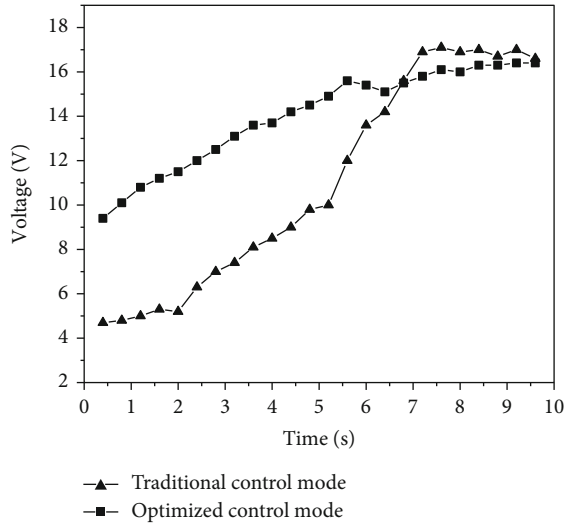


Figure 31: Voltage comparison during MPPT.

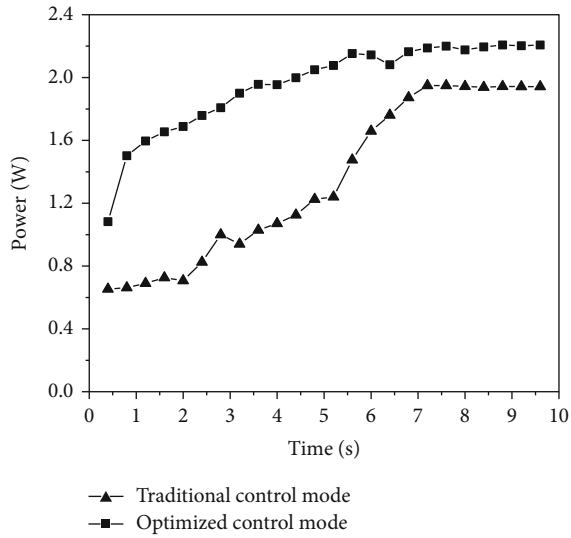


Figure 32: Output power comparison during MPPT.

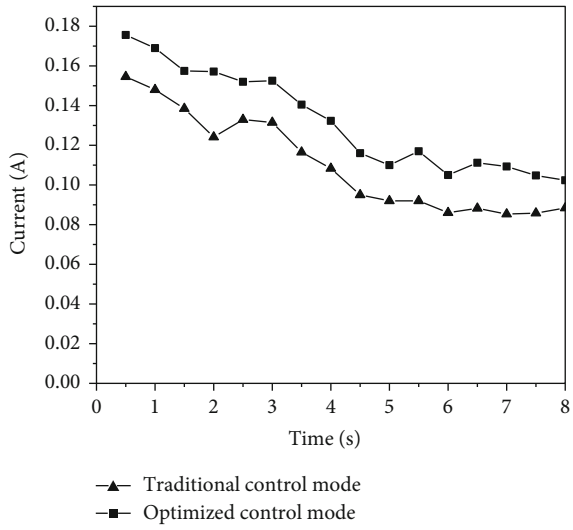


Figure 33: Current comparison during MPPT.

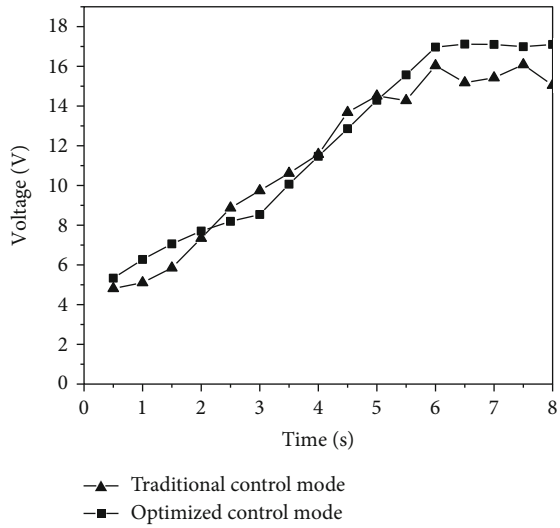


Figure 34: Voltage comparison during MPPT.

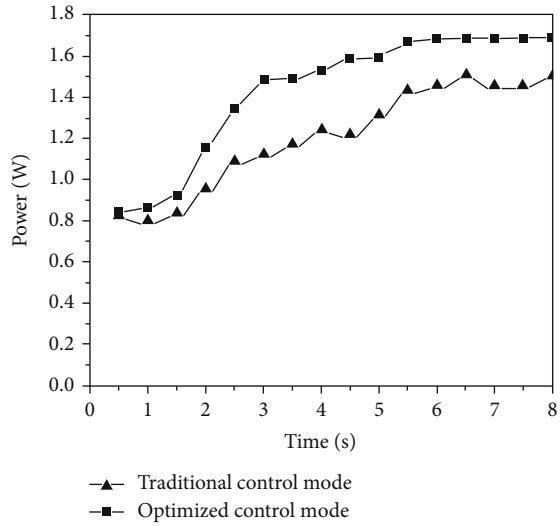


Figure 35: Output power comparison during MPPT.

Figure 28, the curve finally converges around 1.94 W, indicating that the PV optimizer can quickly and accurately track and control the MPP when the monolithic PV module is shaded.

Experiment 2 was carried out on the basis of Experiment 1. Two PV modules were used, and one BOOST circuit was connected in series behind each PV module in Experiment 2. The shadow occlusion conditions of the two PV modules and the MPPT control mode are shown in Figure 29. During the experiment, the irradiance of PV module 1 was 770 W/m$^2$, and that of PV module 2 was 475 W/m$^2$, which was the same as that of Experiment 1, that is, PV module 2 was affected by the shadow blocking. The current comparison, voltage comparison, and output power comparison between the traditional MPPT control mode and the optimized MPPT control mode are illustrated in Figures 30–32, respectively.

According to Figure 32, the output power of the two PV modules in the traditional MPPT control mode is 1.94 W, and the output power in the optimized MPPT control mode is 2.20 W, an efficiency increase of 13.4%. The PV optimizer eliminates energy losses due to uneven illumination and component mismatch, realizes decoupling between the controls of the PV cells, and optimizes the output power of the monolithic PV panels. Figure 30 clearly shows that the current of the traditional MPPT control mode is smaller than that of the optimized control mode, and when the MPP is traced, the voltage value in the traditional control mode and the optimized control mode is basically the same (see Figure 31), so increasing the current can produce a remarkable efficiency improvement of the PV strings.

Based on the above experiments, the difference in irradiance between the two PV modules has been reduced. The irradiance of PV module 1 was 600 W/m$^2$, and that of PV

module 2 was 450 W/m$^2$. The experimental results are shown in Figures 33–35.

As depicted in Figure 35, the output power of the traditional MPPT control mode is 1.50 W, and the output power of the optimized MPPT control mode is 1.69 W, an efficiency increase of 12.7%. This efficiency improvement is less than 13.4% (see Figure 32), which is due to the decrease of the irradiance gap.

The experimental data comparison has shown that optimized MPPT control mode can increase the output power of the PV module under PSCs more efficiently. In terms of economy, this model will increase the production cost of PV modules, but with the development of power electronics integration technology, the economic benefits of improving the output efficiency of PV modules will be greater.

## 7. Conclusion

Shading and mismatching create an urgent problem for PV power plants, and they have always been hot issues in the field of PV research. Based on the five-parameter model, a multipeak output model is proposed. By comparing the simulation data with the experimental data, the relative errors of the output power at the peak points in these $P - V$ curves are all within 2.1%.

An OPSO algorithm is proposed to track the GMPP under PSCs, and the convergence speed of the OPSO algorithm is more than twice as fast as that of the traditional PSO algorithm when the output power of PV modules reached convergence. Furthermore, based on the multipeak output model and the OPSO algorithm, a PV optimizer is proposed to solve the problem of shading and mismatch in PV systems, including the hardware design and software programming. The experimental results demonstrate that the PV optimizer can produce a remarkable efficiency improvement of the PV strings under the PSC by 13.4%. These results lay a foundation for the development of intelligent PV modules.

## Abbreviations

PSCs: Partial shading conditions
PSO: Particle swarm optimization
OPSO: Optimized particle swarm optimization
MPP: Maximum power point
GMPP: Global maximum power point
INC: Incremental conductance
FA: Firefly algorithm
DE: Differential evolutionary
GA: Genetic algorithm
CV: Constant voltage
FOCV: Fractional open-circuit voltage
FSCC: Fractional short-circuit current
P&O: Perturb and observe
CS: Cuckoo search
GWO: Grey wolf optimization
MRL: Memetic reinforcement learning
DLCI: Dynamic leader based collective intelligence
MSSA: Memetic salp swarm algorithm
NOCT: Nominal operating cell temperature.

*PV System Parameters*

$P_m$: Power at MPP (W)
$V_m$: Voltage at MPP (V)
$I_m$: Current at MPP (A)
$V_{oc}$: Open-circuit voltage of the PV modules (V)
$I_{sc}$: Short-circuit current of the PV modules (A)
$\eta_m$: PV battery conversion efficiency (%)
$u_{I,sc}$: Temperature coefficient of the short-circuit current (%/°C)
$u_{V,oc}$: Temperature coefficient of the open-circuit voltage (%/°C)
$T_{NOCT}$: Cell temperature at NOCT (°C).

## Data Availability

The data used to support the findings of this study are available from the corresponding author upon request.

## Conflicts of Interest

The authors declare that they have no conflicts of interest to this work.

## Acknowledgments

This research work presented in this paper was financially supported by the National Natural Science Foundation of China, No. 51676063.

## References

[1] C. Deline, "Partially shaded operation of a grid-tied PV system," in *Conference Record of the IEEE Photovoltaic Specialists Conference*, pp. 1268–1273, 2009.

[2] F. Martínez-Moreno, J. Muñoz, and E. Lorenzo, "Experimental model to estimate shading losses on PV arrays," *Solar Energy Materials and Solar Cells*, vol. 94, no. 12, pp. 2298–2303, 2010.

[3] M. C. Alonso-García, W. Herrmann, W. Böhmer, and B. Proisy, "Thermal and electrical effects caused by outdoor hot-spot testing in associations of photovoltaic cells," *Progress in Photovoltaics: Research and Applications*, vol. 11, no. 5, pp. 293–307, 2003.

[4] M. A. Elgendy, B. Zahawi, and D. J. Atkinson, "Assessment of perturb and observe MPPT algorithm implementation techniques for PV pumping applications," *IEEE Transactions on Sustainable Energy*, vol. 3, no. 1, pp. 21–33, 2012.

[5] D. Sera, L. Mathe, T. Kerekes, S. V. Spataru, and R. Teodorescu, "On the perturb-and-observe and incremental conductance mppt methods for PV systems," *IEEE Journal of Photovoltaics*, vol. 3, no. 3, pp. 1070–1078, 2013.

[6] A. Safari and S. Mekhilef, "Simulation and hardware implementation of incremental conductance MPPT with direct control method using cuk converter," *IEEE Transactions on Industrial Electronics*, vol. 58, no. 4, pp. 1154–1161, 2011.

[7] K. A. Aganah and A. W. Leedy, "A constant voltage maximum power point tracking method for solar powered systems," in *Proceedings of the Annual Southeastern Symposium on System Theory*, pp. 125–130, 2011.

[8] D. Baimel, R. Shkoury, L. Elbaz, S. Tapuchi, and N. Baimel, "Novel optimized method for maximum power point tracking in PV systems using fractional open circuit voltage technique," *2016 International Symposium on Power Electronics, Electrical Drives, Automation and Motion, SPEEDAM*, vol. 2, pp. 889–894, 2016.

[9] H. A. Sher, A. F. Murtaza, A. Noman, K. E. Addoweesh, and M. Chiaberge, "An intelligent control strategy of fractional short circuit current maximum power point tracking technique for photovoltaic applications," *Journal of Renewable and Sustainable Energy*, vol. 7, no. 1, 2015.

[10] P. Samantaray and S. Sasmita, "Performance of solar photovoltaic module under partial shading conditions," in *Proceedings of the 10th International Conference on Intelligent Systems and Control, ISCO 2016*, pp. 1–4, 2016.

[11] V. Quaschning and R. Hanitsch, "Numerical simulation of current-voltage characteristics of photovoltaic systems with shaded solar cells," *Solar Energy*, vol. 56, no. 6, pp. 513–520, 1996.

[12] A. S. Masoum, F. Padovan, and M. A. S. Masoum, "Impact of partial shading on voltage- and current-based maximum power point tracking of solar modules," in *IEEE PES General Meeting*, pp. 1–5, 2010.

[13] M. A. Danandeh and M. G. SM, "Comparative and comprehensive review of maximum power point tracking methods for PV cells," *Renewable and Sustainable Energy Reviews*, vol. 82, pp. 2743–2767, 2018.

[14] D. Picault, B. Raison, and S. Bacha, "Reducing mismatch losses in grid-connected residential BIPV arrays using active power conversion components," in *European Photovoltaic Solar Energy Conference*, 2010.

[15] Y. H. Ji, D. Y. Jung, J. G. Kim, J. H. Kim, T. W. Lee, and C. Y. Won, "A real maximum power point tracking method for mismatching compensation in PV array under partially shaded conditions," *IEEE Transactions on Power Electronics*, vol. 26, no. 4, pp. 1001–1009, 2011.

[16] K. S. Tey and S. Mekhilef, "Modified incremental conductance algorithm for photovoltaic system under partial shading conditions and load variation," *IEEE Transactions on Industrial Electronics*, vol. 61, no. 10, pp. 5384–5392, 2014.

[17] K. Hu, S. Cao, W. Li, and F. Zhu, "An improved particle swarm optimization algorithm suitable for photovoltaic power tracking under partial shading conditions," *IEEE Access*, vol. 7, pp. 143217–143232, 2019.

[18] T. Sen, N. Pragallapati, V. Agarwal, and R. Kumar, "Global maximum power point tracking of PV arrays under partial shading conditions using a modified particle velocity-based PSO technique," *IET Renewable Power Generation*, vol. 12, no. 5, pp. 555–564, 2018.

[19] B. R. Peng, K. C. Ho, and Y. H. Liu, "A novel and fast MPPT method suitable for both fast changing and partially shaded conditions," *IEEE Transactions on Industrial Electronics*, vol. 65, no. 4, pp. 3240–3251, 2018.

[20] D. F. Teshome, C. H. Lee, Y. W. Lin, and K. L. Lian, "A modified firefly algorithm for photovoltaic maximum power point tracking control under partial shading," *IEEE Journal of Emerging and Selected Topics in Power Electronics*, vol. 5, no. 2, pp. 661–671, 2017.

[21] L. P. Sampaio, M. V. Da Rocha, S. A. O. Da Silva, and M. H. T. De Freitas, "Comparative analysis of MPPT algorithms bio-inspired by grey wolves employing a feed-forward control loop in a three-phase grid-connected photovoltaic system," *IET Renewable Power Generation*, vol. 13, no. 8, pp. 1379–1390, 2019.

[22] K. S. Tey, S. Mekhilef, M. Seyedmahmoudian, B. Horan, A. T. Oo, and A. Stojcevski, "Improved differential evolution-based MPPT algorithm using SEPIC for PV systems under partial shading conditions and load variation," *IEEE Transactions on Industrial Informatics*, vol. 14, no. 10, pp. 4322–4333, 2018.

[23] S. Daraban, D. Petreus, and C. Morel, "A novel MPPT (maximum power point tracking) algorithm based on a modified genetic algorithm specialized on tracking the global maximum power point in photovoltaic systems affected by partial shading," *Energy*, vol. 74, pp. 374–388, 2014.

[24] M. Seyedmahmoudian, B. Horan, T. K. Soon et al., "State of the art artificial intelligence-based MPPT techniques for mitigating partial shading effects on PV systems - a review," *Renewable and Sustainable Energy Reviews*, vol. 64, pp. 435–455, 2016.

[25] X. Zhang, S. Li, T. He et al., "Memetic reinforcement learning based maximum power point tracking design for PV systems under partial shading condition," *Energy*, vol. 174, pp. 1079–1090, 2019.

[26] B. Yang, T. Yu, X. Zhang et al., "Dynamic leader based collective intelligence for maximum power point tracking of PV systems affected by partial shading condition," *Energy Conversion and Management*, vol. 179, pp. 286–303, 2019.

[27] B. Yang, L. Zhong, X. Zhang et al., "Novel bio-inspired memetic salp swarm algorithm and application to MPPT for PV systems considering partial shading condition," *Journal of Cleaner Production*, vol. 215, pp. 1203–1222, 2019.

[28] W. Zha1ng, G. Zhou, H. Ni, and Y. Sun, "A modified hybrid maximum power point tracking method for photovoltaic arrays under partially shading condition," *IEEE Access*, vol. 7, pp. 160091–160100, 2019.

[29] H. Li, D. Yang, W. Su, J. Lu, and X. Yu, "An overall distribution particle swarm optimization MPPT algorithm for photovoltaic system under partial shading," *IEEE Transactions on Industrial Electronics*, vol. 66, no. 1, pp. 265–275, 2019.

[30] M. Seyedmahmoudian, R. Rahmani, S. Mekhilef et al., "Simulation and hardware implementation of new maximum power point tracking technique for partially shaded PV system using hybrid DEPSO method," *IEEE Transactions on Sustainable Energy*, vol. 6, no. 3, pp. 850–862, 2015.

[31] M. Kermadi, Z. Salam, J. Ahmed, and E. M. Berkouk, "An effective hybrid maximum power point tracker of photovoltaic arrays for complex partial shading conditions," *IEEE Transactions on Industrial Electronics*, vol. 66, no. 9, pp. 6990–7000, 2019.

[32] S. Mohanty, B. Subudhi, and P. K. Ray, "A grey wolf-assisted perturb & observe MPPT algorithm for a PV system," *IEEE Transactions on Energy Conversion*, vol. 32, no. 1, pp. 340–347, 2017.

[33] J. Y. Shi, L. T. Ling, F. Xue et al., "Combining incremental conductance and firefly algorithm for tracking the global MPP of PV arrays," *Journal of Renewable and Sustainable Energy*, vol. 9, no. 2, 2017.

[34] D. A. Nugraha, K. L. Lian, and S. Suwarno, "A novel mppt method based on cuckoo search algorithm and golden section search algorithm for partially shaded pv system," *Canadian Journal of Electrical and Computer Engineering*, vol. 42, no. 3, pp. 173–182, 2019.

[35] J. Bai, S. Liu, Y. Hao, Z. Zhang, M. Jiang, and Y. Zhang, "Development of a new compound method to extract the five

parameters of PV modules," *Energy Conversion and Management*, vol. 79, pp. 294–303, 2014.

[36] J. Bai, Y. Cao, Y. Hao, Z. Zhang, S. Liu, and F. Cao, "Characteristic output of PV systems under partial shading or mismatch conditions," *Solar Energy*, vol. 112, pp. 41–54, 2015.

[37] A. Khare and S. Rangnekar, "A review of particle swarm optimization and its applications in Solar Photovoltaic system," *Applied Soft Computing Journal*, vol. 13, no. 5, pp. 2997–3006, 2013.

[38] Y. Shi and R. Eberhart, "A modified particle swarm optimizer algorithm," in *1998 IEEE International Conference on Evolutionary Computation Proceedings, IEEE World Congress on Computational Intelligence*, pp. 69–73, 1998.

[39] J. S. Arora, *Introduction to Optimum Design*, Elsevier, 2016.

[40] H. Patel and V. Agarwal, "Maximum power point tracking scheme for PV systems operating under partially shaded conditions," *IEEE Transactions on Industrial Electronics*, vol. 55, no. 4, pp. 1689–1698, 2008.

[41] R. C. Eberhart and Y. Shi, "Tracking and optimizing dynamic systems with particle swarms," *Proceedings of the IEEE Conference on Evolutionary Computation*, vol. 1, pp. 94–100, 2001.